13th World Conference on Earthquake Engineering
Vancouver, B.C., Canada
August 1-6, 2004
Paper No. 2934

EFFECTS OF THE VERTICAL ACCELERATION ON THE RESPONSE OF BASE-ISOLATED STRUCTURES SUBJECTED TO NEAR-FAULT GROUND MOTIONS

Fabio MAZZA[1] and Alfonso VULCANO[2]

SUMMARY

The main objective of this work is to investigate the effects due to the combination of the vertical and horizontal components of near-fault ground motions on the nonlinear dynamic response of base-isolated structures. To this aim, a numerical investigation is carried out with reference to a base-isolated five-storey reinforced concrete (r.c.) framed building, designed according to Eurocode 8 (EC8) provisions. The design of the test structures is carried out considering only the horizontal seismic loads evaluated in a high-risk region, with reference to the subsoil classes A and D (corresponding to rock and moderately soft soil, respectively). A bilinear model idealizes the behaviour of a r.c. frame member, while for an isolator, i.e. high-damping-laminated-rubber bearing, a viscoelastic linear model is adopted. The seismic analysis of the test structures is carried out by using a step-by-step procedure, considering horizontal and vertical components of near-fault ground motions with different values of the ratio between the peak value of the vertical acceleration and the analogous value of a horizontal component of acceleration.

INTRODUCTION

The insertion of an isolation system at the base of a building structure allows to reduce the horizontal seismic loads through a decoupling of the structure motion from that of the soil; moreover, the structure behaves like a fixed-base structure towards the vertical seismic loads, as a consequence of the high stiffness of the isolators in the vertical direction. During near-fault ground motions, even base-isolated structures designed according to recent seismic codes can undergo unforeseen structural damages.

Particular attention was paid by many authors (e.g., Alaghebandian et al. [1] and Decanini et al. [2]) to study the effects of the vertical component of near-fault ground motions on the nonlinear response of fixed-base structures. On the contrary, little attention was addressed to studying the effects of the above motion component on the behaviour of base-isolated structures; however, isolation systems effective also in the vertical direction have been proposed for nuclear plants (Morishita et al. [3]). Therefore, it is

[1] Research Assistant, Dipartimento di Strutture, Università della Calabria, Arcavacata di Rende (Cosenza), Italy. Email: fmazza@unical.it
[2] Professor, Dipartimento di Strutture, Università della Calabria, Arcavacata di Rende (Cosenza), Italy. Email: vulcano@unical.it

believed very important to check the effectiveness of the base isolation considering the combined effects of the horizontal and vertical components of near-fault ground motions.

The near-fault ground motions are generally characterized by long-period horizontal pulses and high values of the ratio between the peak value of the vertical acceleration, PGA_V, and the analogous value of the horizontal acceleration, PGA_H (Kelly [4], Benedetti et al. [5]). High values of the above acceleration ratio (PGA_V/PGA_H) can notably modify the axial load in the columns, producing undesirable phenomena in these elements (Papazoglou et al. [6]): e.g., brittle failure in compression or failure under a relatively high tensile load, buckling of the longitudinal bars. Moreover, base-isolated structures are generally designed assuming that the effects due to the vertical seismic loads are negligible in comparison with those due to the horizontal ones (e.g., as in Eurocode 8 [7], at least with reference to far-fault earthquakes). But the concurrent action of the vertical and horizontal seismic loads can produce inelastic deformations of the superstructure; then, it is also possible an amplification of the structural response due to the long duration of a horizontal pulse.

The above considerations emphasize the need of investigating the seismic behaviour of base-isolated structures located near faults, considering the horizontal and vertical components of the ground motion acting simultaneously. To this aim, a numerical investigation is carried out with reference to a typical base-isolated five-storey r.c. framed building, designed according to the provisions of EC8. In this study high-damping-laminated-rubber bearings (HDLRBs) are considered as isolators. Base-isolated test structures are designed assuming different values of the fundamental vibration period and considering two subsoil classes, A and D (corresponding to rock and moderately soft soil, respectively), in a high-risk region. The nonlinear dynamic response of the test structures is analyzed under ground motions assumed, with different values of the acceleration ratio (PGA_V/PGA_H), on the basis of motions recorded near-faults in Turkey (1999, 2003) and Greece (1986, 1999).

NEAR-FAULT GROUND MOTIONS

The seismic response depends on the interaction between the characteristics of the structure and those of the ground motion (frequency content, intensity, duration, etc.). In particular, near-fault earthquakes are characterized by both long-duration pulses along horizontal directions and high-frequency motion in the vertical direction. The insertion of an isolation system at the base of a structure produces (in comparison with the fixed-base structure) a large increase of its horizontal deformability, which can give rise to an amplification of the structural response during near-fault earthquakes. Moreover, this amplification can be emphasized due the combination of the actions produced by the horizontal and vertical components of the ground motion; in addition, in the vertical direction a base-isolated structure behaves like a fixed-base and exhibits a low damping capacity.

Some seismic codes (e.g., those adopted in Mexico and U.S.A.) adopt a design value of the peak vertical acceleration, PGA_V, related to the analogous value of the peak horizontal acceleration, PGA_H (Salazar et al. [8]). For instance, EC8 adopts, in a high-risk seismic region (magnitude M_s>5.5), an acceleration ratio α_{PGA}(=PGA_V/PGA_H), assuming different values depending on the subsoil class: e.g., the maximum value 0.9, in the case of rock (class A); the value 2/3, in the case of moderately soft soil (class D). Nevertheless, strong ground motions recorded near a fault showed even values $\alpha_{PGA}>1$, different from the values assumed in EC8 with reference to far-fault ground motions. To emphasize that, the main data of strong near-fault earthquakes are shown in table 1: i.e., recording station; peak vertical acceleration (PGA_V); maximum peak value of the horizontal acceleration components ($PGA_{H,max}$); acceleration ratio α_{PGA}(=$PGA_V/PGA_{H,max}$). It is noteworthy that α_{PGA} presents a large variability, going from a minimum of 0.61 for the Athens earthquake (1999) to a maximum of 2.43 for the Nahanni earthquake (1985).

Table 1: Acceleration components of near-fault earthquakes and corresponding acceleration ratio α_{PGA}(=$PGA_V/PGA_{H,max}$).

Nation	Earthquake	Station	PGA_V	$PGA_{H,max}$	α_{PGA}
Greece	Kalamata, 1986	OTE-Building	0.33g	0.30g	1.10
	Athens, 1999	Sepolia	0.20g	0.33g	0.61
Iran	Tabas, 1978	Tabas	0.69g	0.85g	0.81
Turkey	Izmit, 1999	Izmit	0.14g	0.22g	0.64
	Izmit, 1999	Yarimca-Petkim	0.24g	0.30g	0.77
	Duzce, 1999	Mudurlugu	0.34g	0.51g	0.67
	Bingol, 2003	Bayindirlik	0.45g	0.52g	0.87
California	Imperial Valley, 1979	Agrarias	0.83g	0.37g	2.24
	Loma Prieta, 1989	Los Gatos	0.60g	0.89g	1.47
	Landers, 1992	Lucerne	0.86g	0.81g	1.06
	Northridge, 1994	Rinaldi	0.85g	0.47g	1.81
Canada	Nahanni, 1985	Station 1	2.37g	1.35g	2.43
Japan	Kobe, 1995	Port Island Array	0.57g	0.35g	1.63

At present, EC8 requires to adopt specific response spectra for the design of base-isolated structures in the case the design PGA_V value be greater than 0.25g. Moreover, specific response spectra are required only for particular isolated structures (i.e., hospitals, nuclear plants, etc.), located at less than 15 km from the nearest fault potentially active for which a magnitude $M_s \geq 6.5$ is expected.

To study the seismic response of the test structures, which will be described in the next section, near-fault motions recorded in Turkey (1999, 2003) and Greece (1986, 1999), whose data are available in the European Strong motion Database developed by the European Commission for Community Research [9], are considered. The main data of the motions recorded in Turkey, which proved to be the most severe for the examined structures, are shown in table 2, where are reported: recording station and its distances from the epicentre (Δ_e) and the fault (Δ_f); soil type; magnitude (M_w); peak values attained by the vertical acceleration component (PGA_V) and the two horizontal acceleration components (PGA_{N-S} and PGA_{E-W}).

Table 2: Main data of near-fault ground motions recorded in Turkey.

Earthquake	Station	Δ_e (km)	Δ_f (km)	Soil	M_w	PGA_V	PGA_{N-S}	PGA_{E-W}
Izmit, 17/8/1999	Izmit	9	5	rock	7.6	0.14g	0.16g	0.22g
Bingol, 1/5/2003	Bayindirlik	14	-	rock	6.3	0.45g	0.52g	0.30g
Izmit-YP, 17/8/1999	Yarimca-Petkim	20	5	soft	7.6	0.24g	0.30g	0.24g
Duzce, 12/11/1999	Mudurlugu	8	0	soft	7.2	0.34g	0.38g	0.51g

The elastic spectral values obtained, with reference to the horizontal components of the ground motions considered in table 2, for the absolute input energy for unit of mass (Uang et al. [10]) and for the horizontal acceleration components are shown in figures 1 and 2, separately for the two considered classes of soil. All the above spectral values have been obtained for vibration periods $T \leq 5$ s, assuming a viscous-damping factor ξ=0.12, to account globally for the damping contributions due to the isolation system (10%) and the superstructure (2%) with reference to a horizontal motion. Analogous spectral values, for vibration periods $T \leq 1$ s, are shown in figure 3 with reference to the vertical component of the ground motions considered in table 2, but in this case it is assumed ξ=0.02, because of the low damping capacity of the isolated structure expected in the vertical direction. In all the above figures are also shown the curves based on the EC8 spectra in a high-risk region for rock (EC8.A; PGA_H=0.35g and PGA_V=0.32g) and moderately soft soil (EC8.D; PGA_H=0.47g and PGA_V=0.32g); in particular, the input energy spectra have been obtained by using artificially generated accelerograms.

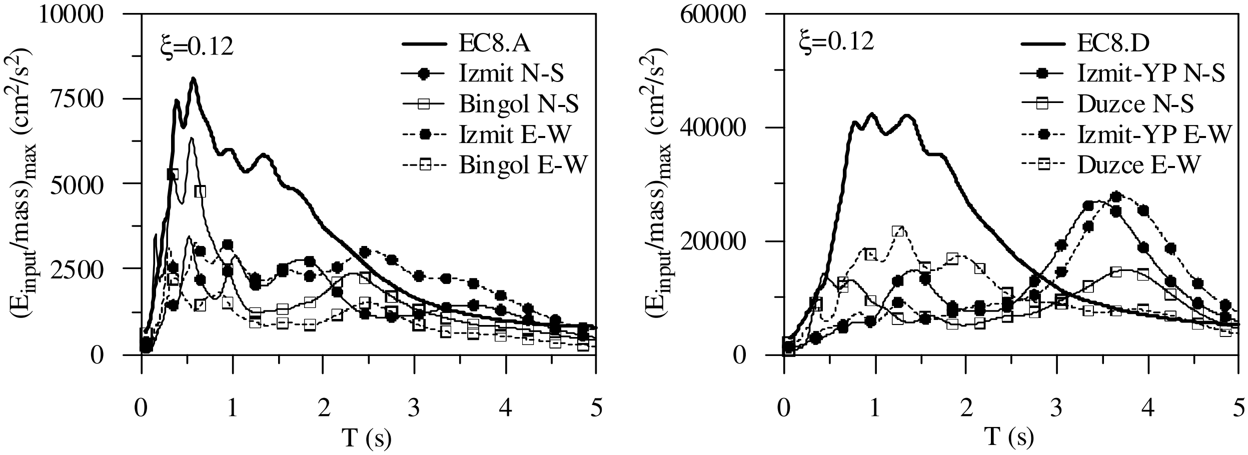

(a) Rock. **(b) Moderately soft soil.**

Figure 1: Elastic response spectra of the absolute input energy for the horizontal acceleration components.

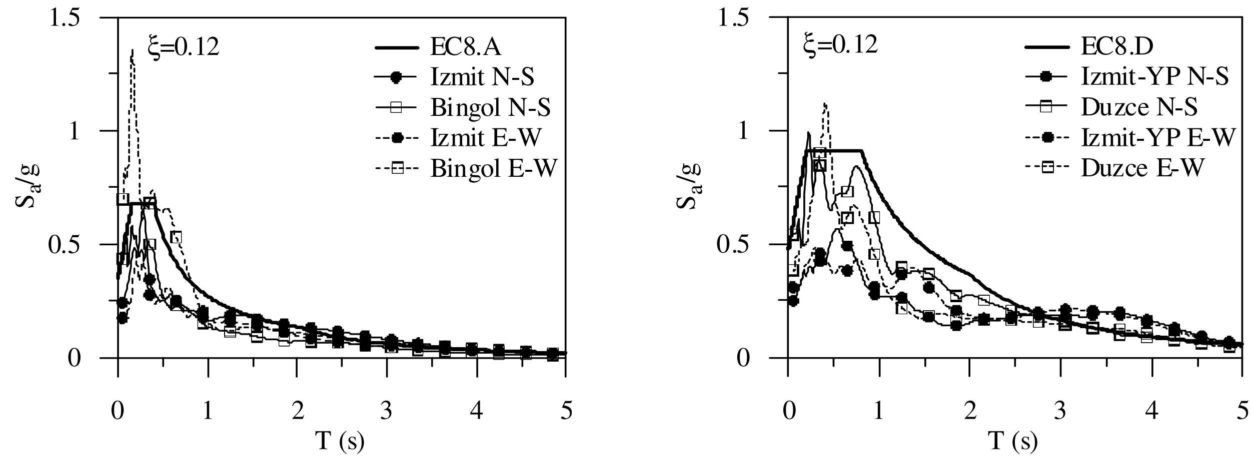

(a) Rock. **(b) Moderately soft soil.**

Figure 2: Elastic response spectra for the horizontal acceleration components.

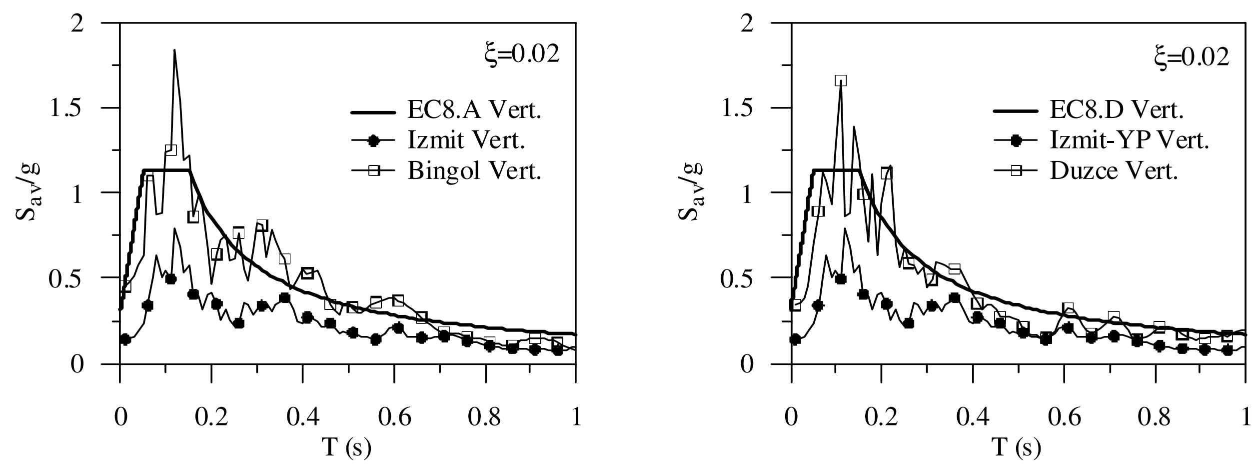

(a) Rock. **(b) Moderately soft soil.**

Figure 3: Elastic response spectra for the vertical acceleration component.

TEST STRUCTURES

A typical five-storey residential building, with a r.c. framed structure isolated at the base by HDLRBs, is considered for the numerical investigation. The plan of the r.c. framed structure is shown in figure 4a, while in figure 4b it is reported the plane base-isolated frame which will be considered as a reference scheme for the test structures examined in the numerical investigation.

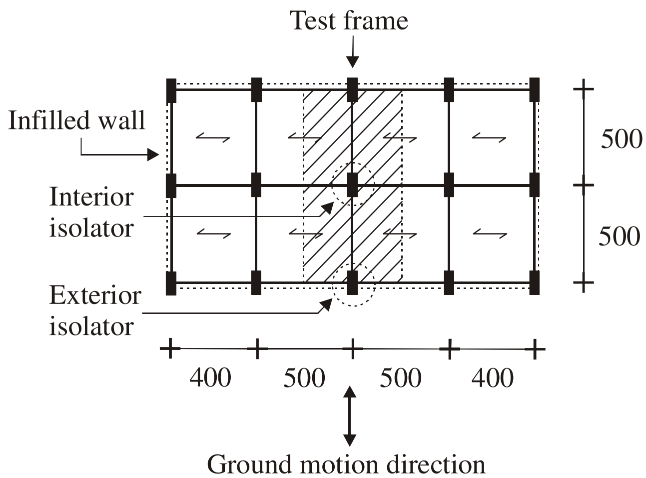

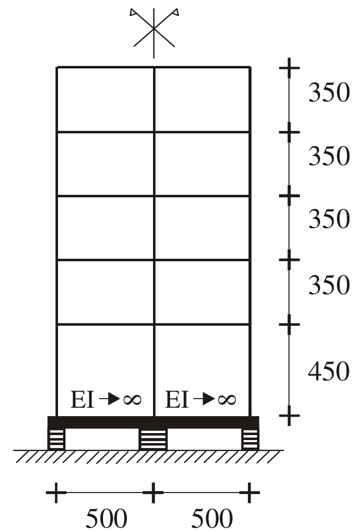

(a) Plan of the r.c. framed structure. (b) Reference plane base-isolated frame.

Figure 4: Test structure (dimensions in cm).

The proportioning of the test structures has been done considering only the horizontal seismic actions according to EC8, assuming: “full isolation” (i.e., the behaviour factor is assumed as to be q=1); high-risk region with magnitude M_s>5.5 (PGA_H=0.35g or 0.47g, respectively for subsoil class A or D). In the design of the structure, the vertical component of the ground motion is neglected: this assumption, according to seismic rules recently enacted in Italy (Ordinanza no. 3274 [11]), is acceptable provided that the HDLRBs be characterized by a stiffness ratio $\alpha_K(=K_V/K_H$, being K_V and K_H the vertical stiffness and the horizontal one, respectively) not less than 800.

More precisely, six cases are considered, with reference to three values of the fundamental vibration period of the isolated structure (T_I=2s, 3s and 4s) for each of the two considered subsoil classes (A and D). Each base-isolated structure (BI) is identified by two characters following the acronym BI: the first one (2, 3 or 4) refers to the T_I value in seconds, while the second one (A or D) to the subsoil class. Further detail regarding the geometric and mechanical characteristics of the test structures can be found in another paper aimed to compare different base-isolation techniques (Mazza et al. [12]).

The masses of the dead loads and those of the quasi-permanent live loads are assumed according to EC8. In particular, at each floor of the isolated frame in figure 4b, the following masses are considered: lumped masses at the interior joints (m_i) and exterior ones (m_e), representing the contribution of the transverse girders and, in case, of the masonry infills; uniformly distributed mass along the girders (μ_g) and columns (μ_c), corresponding to the gravity load of the considered structural member and, in the case of a girder, also of the floor slab. Lumped and distributed masses equal to 1.5 times those of the first floor are assumed at the level of the base girder placed on the isolators, which is in turn assumed infinitely rigid. In tables 3 and 4 are reported, respectively, the values of the lumped masses and those of the distributed ones, while in table 5 are shown the dimensions of the cross-sections of the girders and columns of the test structures. Lastly, in table 6 are reported the horizontal stiffness (K_H) and the equivalent damping coefficient (C_H) of the isolators, both evaluated with reference to the (horizontal) design displacement according to EC8. The vertical stiffness of the isolators (K_V) is calculated by the following expression suggested in the Ordinanza [11] mentioned above:

$$K_V = \frac{K_H}{\frac{1}{6S_1^2} + \frac{4G}{3E_b}}$$

where S_1 is a shape factor of the isolator, while E_b and G represent, respectively, the compression modulus and the shear modulus of the rubber. In the numerical analyses the isolators are assumed deformable (with a stiffness ratio α_K=1000) or rigid (i.e., $\alpha_K \rightarrow \infty$) in the vertical direction. In particular, when assuming α_K=1000 and neglecting the axial deformability of the columns, the fundamental vibration periods of the test structures with reference to the vertical direction (T_{Iv}), approximately evaluated idealizing the isolated structure as an equivalent single-degree-of-freedom system, are: 0.063s, 0.095s and 0.126s, respectively for the structures BI2.A(D), BI3.A(D) and BI4.A(D).

Table 3: Masses lumped at the exterior joints (m_e) and interior ones (m_i) of the test structures.

	m_e (kNs^2/m)						m_i (kNs^2/m)					
Storey	BI2.A	BI3.A	BI4.A	BI2.D	BI3.D	BI4.D	BI2.A	BI3.A	BI4.A	BI2.D	BI3.D	BI4.D
5	2.20	2.60	2.60	2.87	2.60	2.60	2.20	2.60	2.60	2.87	2.60	2.60
4	7.00	6.73	6.73	7.26	6.99	6.73	2.87	2.60	2.60	3.13	2.87	2.60
3	7.26	6.99	6.86	7.53	7.26	6.99	3.13	2.87	2.73	3.40	3.13	2.87
2	7.53	6.99	6.99	8.03	7.53	6.99	3.40	2.87	2.87	3.90	3.40	2.87
1	7.89	7.64	7.30	9.10	7.99	7.64	3.86	3.52	3.17	4.97	3.86	3.52

Table 4: Masses distributed along the girders (μ_g) and the columns (μ_c) of the test structures.

	μ_g (kNs^2/m^2)						μ_c (kNs^2/m^2)					
Storey	BI2.A	BI3.A	BI4.A	BI2.D	BI3.D	BI4.D	BI2.A	BI3.A	BI4.A	BI2.D	BI3.D	BI4.D
5	2.69	2.69	2.61	2.73	2.61	2.61	0.23	0.23	0.23	0.31	0.23	0.23
4	3.08	3.04	3.04	3.08	3.08	3.04	0.31	0.23	0.23	0.38	0.31	0.23
3	3.08	3.04	3.04	3.16	3.08	3.04	0.38	0.31	0.27	0.46	0.38	0.31
2	3.16	3.04	3.04	3.31	3.16	3.04	0.46	0.31	0.31	0.61	0.46	0.31
1	3.16	3.04	3.04	3.41	3.16	3.04	0.46	0.38	0.31	0.71	0.46	0.38

Table 5: Dimensions (in cm) of the cross-sections of the r.c. members of the test structures.

	Girders					
Storey	BI2.A	BI3.A	BI4.A	BI2.D	BI3.D	BI4.D
5	30x45	30x45	30x45	30x50	30x45	30x45
4	30x50	30x45	30x45	30x50	30x50	30x45
3	30x50	30x45	30x45	30x60	30x50	30x45
2	30x60	30x45	30x45	40x60	30x60	30x45
1	30x60	30x45	30x45	40x70	30x60	30x45
	Columns					
Storey	BI2.A	BI3.A	BI4.A	BI2.D	BI3.D	BI4.D
5	30x30	30x30	30x30	30x40	30x30	30x30
4	30x40	30x30	30x30	30x50	30x40	30x30
3	30x50	30x40	30x35	30x60	30x50	30x40
2	30x60	30x40	30x40	40x60	30x60	30x40
1	30x60	30x50	30x40	40x70	30x60	30x50

Table 6: Mechanical properties of the isolators.

	K_H (kN/m)			C_H (kNs/m)		
Isolators (HDLRBs)	BI2.A(D)	BI3.A(D)	BI4.A(D)	BI2.A(D)	BI3.A(D)	BI4.A(D)
Exterior	1020	428	233	65	41	30
Interior	2040	856	466	130	82	60

NUMERICAL RESULTS

In order to evaluate the effects produced by the combination of the horizontal and vertical components of near-fault ground motions on the response of base-isolated framed buildings, a numerical investigation has been carried out with reference to the test structures described in the previous section, subjected to ground motions characterized by different values (recorded or amplified) of the acceleration ratio α_{PGA}.

The nonlinear analysis is carried out by a step-by-step procedure based on a two-parameters implicit integration scheme and an initial-stress iterative procedure (Vestroni et al. [13], Mazza et al. [14]). At each step of the analysis, plastic conditions are checked at the end sections of the beams and columns, assuming a bilinear moment-curvature law with a hardening ratio of 2%. However, axial strains are assumed fully elastic, while the shear deformation and the P-Δ effect are neglected; the effect of the axial load on the ultimate bending moment of the columns (M-N interaction) is also considered. The damping matrix is assumed so that: with reference to the horizontal motion, the equivalent viscous damping ratio of the isolation system and the analogous ratio of the superstructure be equal to 10% and 2%, respectively; with reference to the vertical motion, the equivalent viscous damping ratio of the isolated structure be globally equal to 2%. A viscoelastic behaviour is assumed for simulating the response of a HDLRB, which is idealized, with reference to both the horizontal direction and the vertical one, by an elastic spring and a dashpot acting in parallel; in particular, the stiffness of the vertical spring (K_V) is simply assumed to be the same in compression and in tension (if necessary, vertical elements, e.g. chains, with suitable properties may be inserted to supply a HDLRB with adequate stiffness in tension).

In order to emphasize the effects due to the vertical component of a near-fault ground motion, the numerical investigation is carried out with reference to cases in which a horizontal component of that motion (e.g., that showing the larger PGA value) acts: (a) alone; (b) contemporaneously with the corresponding vertical component so as recorded; (c) contemporaneously with the recorded vertical component, amplified according to suitable values of the acceleration ratio α_{PGA} assumed not greater than 2.5 (see values in table 1). For the sake of brevity, only meaningful results, which have been obtained for the test structures on moderately soft soil (BI2.D, BI3.D and BI4.D), are shown, while the analogous results for the test structures on rock (BI2.A, BI3.A and BI4.A), whose response was practically elastic, are omitted.

In figure 5 are shown the curves representing, for each of the three values assumed for the fundamental vibration period of the base-isolated structure (T_I=2s, 3s and 4s), the minimum and maximum values attained by the axial load for the isolators assuming different values of the acceleration ratio α_{PGA} (α_{PGA}=0 corresponds to the case of a horizontal acceleration acting alone), under the N-S and vertical components of the Izmit-YP earthquake (figures 5a and 5b), or the E-W and vertical components of the Duzce earthquake (figures 5c and 5d). In particular, the figures 5a and 5c refer to the interior isolators, while the figures 5b and 5d to the exterior ones, assuming, for all the isolators, α_K=1000 and the positive (negative) sign for a compressive (tensile) axial load.

In all the cases whose results are illustrated in figure 5, the minimum and maximum values of the axial load for the isolators, for increasing values of α_{PGA}, increase rather rapidly and this effect, for a same increase of α_{PGA}, is more evident for the interior isolators (figures 5a and 5c), which have a vertical stiffness K_V twice as large as that of an exterior isolator (figures 5b and 5d). Moreover, it should be noted that the curves obtained for the BI4.D structure do not extend beyond the α_{PGA} value of 1.5, because, assuming a α_{PGA} value large enough (e.g., α_{PGA}=2.0), at least a column attained the ultimate axial load in compression or tension.

It is interesting to note that, when considering the recorded vertical component of the motion (corresponding to α_{PGA}=0.77 or 0.67, respectively for the Izmit-YP earthquake or the Duzce one), the interior isolators are generally compressed, except those of the structures BI3.D and BI4.D under the Duzce earthquake, which undergo very limited tensile load; while the exterior isolators are stretched, although the tensile load is rather limited. Moreover, in the case the vertical component of motion is neglected (α_{PGA}=0), the minimum and maximum axial loads attained by the interior isolators are practically (or exactly) equal to the axial load due to the gravity only, because the axial-load contribution induced by the horizontal seismic loads is negligible (or vanishes, if the framed structure behaves elastically) due to the structural symmetry.

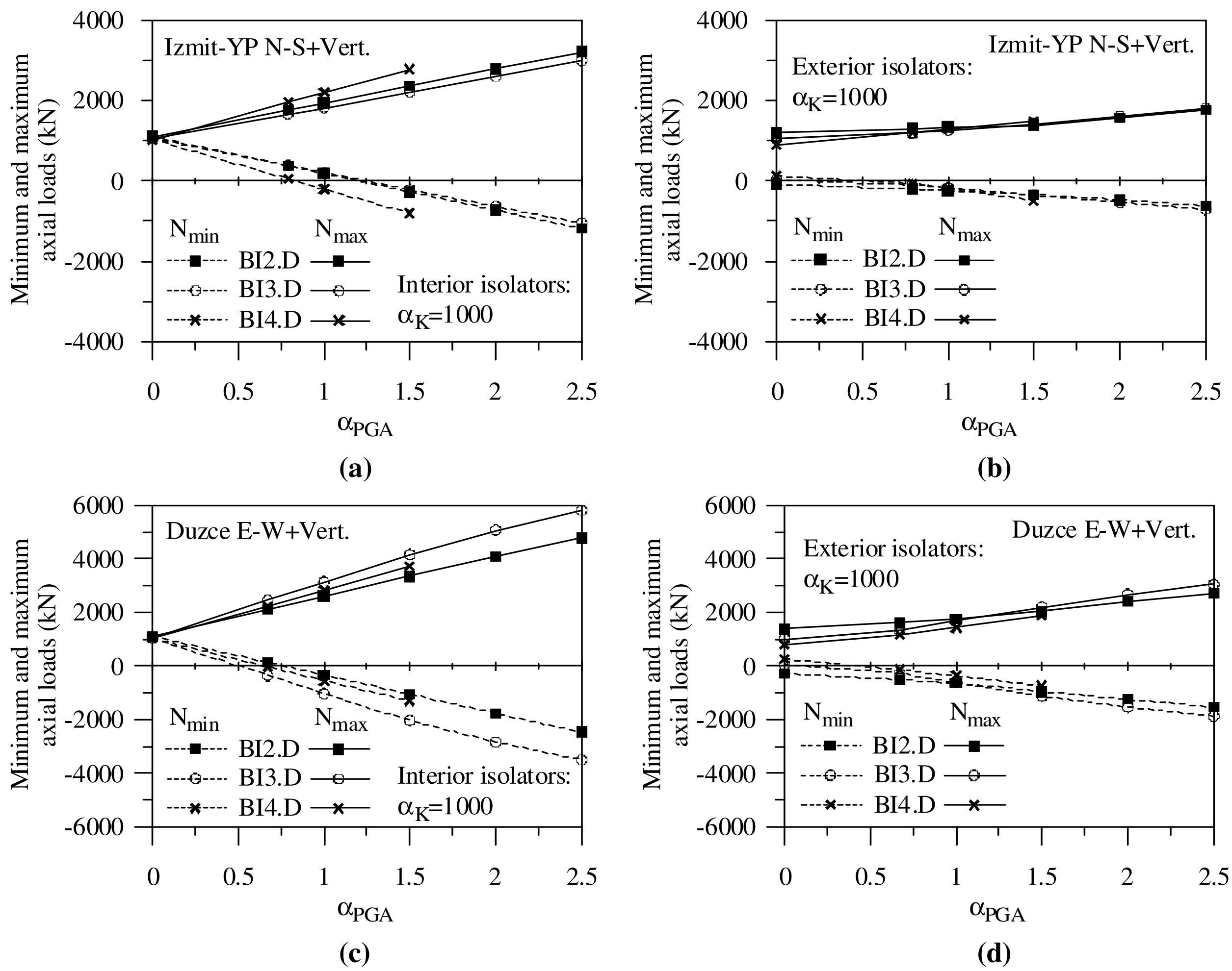

Figure 5: Minimum and maximum axial loads for the isolators assuming different values of the acceleration ratio (α_{PGA}).

Successively, the attention has been focused on the axial load attained by the columns, in order to check if failure phenomena occur: i.e., failure under compression or tension, due to the attainment of the ultimate axial load N_{cu} or N_{tu}, respectively; brittle failure under a compressive load greater than the balanced-failure load N_b. For this purpose, in figure 6 are shown, for different values of α_{PGA}, the minimum (generally, tensile) axial load and the maximum (compressive) one attained by the columns at each storey of the BI4.D structure undergoing severe damages under the near-fault ground motions considered in this study. More precisely, the results, reported for the exterior columns (figures 6a and 6b) and the interior ones (figures 6c and 6d), have been obtained considering the E-W component of the Duzce earthquake, acting alone or in combination with the corresponding vertical component (so as recorded or amplified), and considering the deformability of the isolators (i.e., assuming α_K=1000).

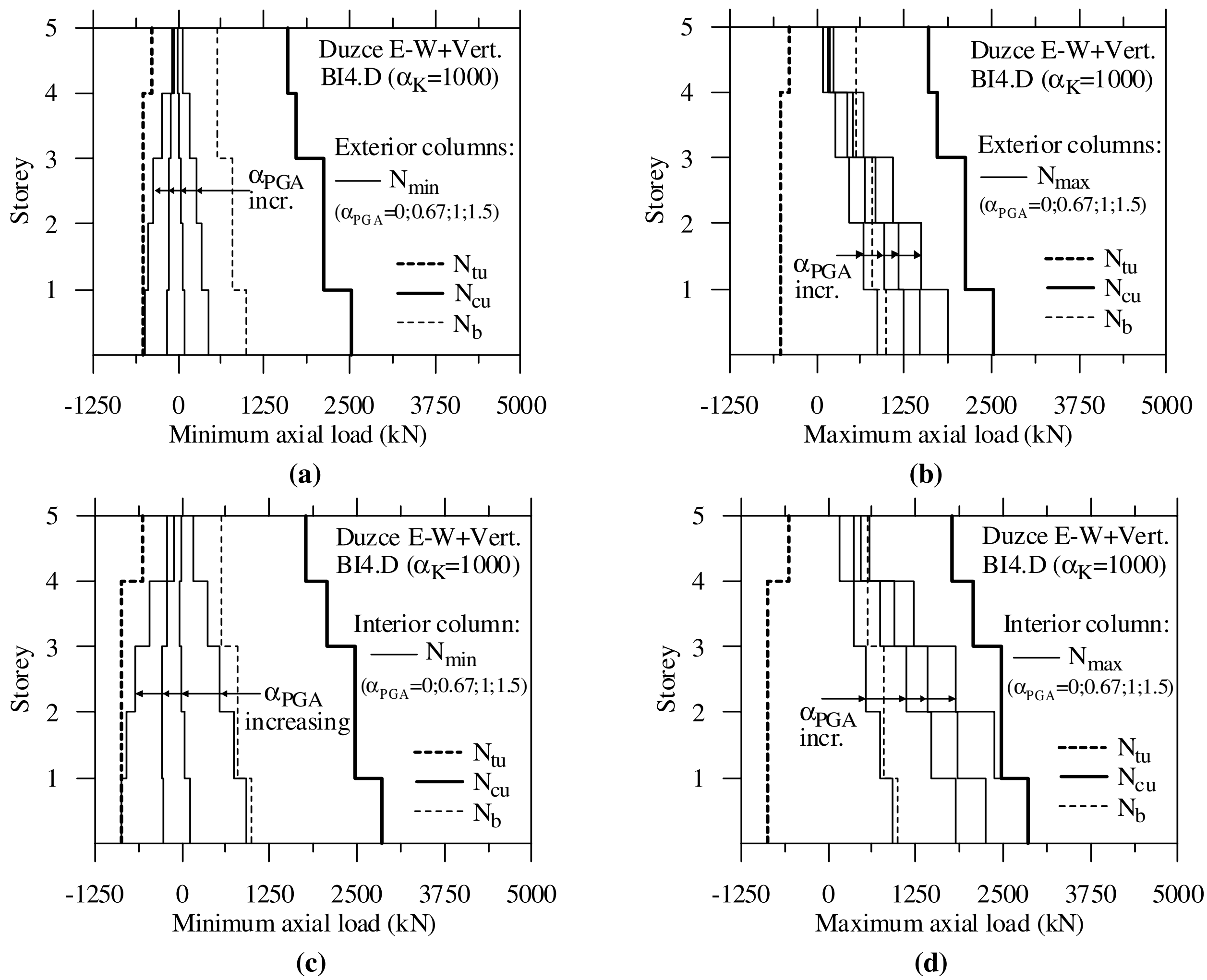

Figure 6: Minimum and maximum axial loads for the columns assuming different values of the acceleration ratio (α_{PGA}).

From the results it comes out that the interior columns undergo more critical conditions than the exterior columns, especially at the lower storeys under a compressive axial load. In particular, for α_{PGA} values large enough (even for the value α_{PGA}=0.67, corresponding to the recorded Duzce motion), the compressive load exceeds the balanced-failure load N_b at each storey, except at the top one. Moreover, when assuming α_{PGA}=1.5, the interior column at the two lower storeys undergo a compressive load and a tensile one very close to the ultimate loads, N_{cu} and N_{tu}, respectively. Analogous results, omitted for the sake of brevity, have been obtained for the columns of the structure BI4.D subjected to the N-S component of the Izmit-YP earthquake acting alone or contemporaneously with the vertical one.

It should be noted that a compressive load greater than N_b does not imply necessarily a brittle failure, because this depends on the value attained by the bending moment, which may be less than the ultimate moment corresponding to the current axial load. Nevertheless, caution is needed when the compressive load is greater than N_b, particularly for base-isolated structures located in regions close to a potentially active fault, also because near-fault earthquakes with an intensity greater than that of the ground motions considered in this study can occur. It is also useful to note that EC8 requires that, in the case of high (medium) ductility class, the maximum compressive load for the columns of fixed-base framed structures be not greater than 55% (65%) of the ultimate load N_{cu}; instead, no analogous prescription is provided in the case of a base-isolated structure.

A confirmation of the importance of considering the effects of the vertical component of near-fault ground motions comes out from the figures 7a and 7b, where it is reported, with reference to the E-W component of the Duzce earthquake acting alone (α_{PGA}=0) or contemporaneously with the recorded vertical one (α_{PGA}=0.67), the time history of the axial load for first-storey columns of the BI4.D structure, when assuming, for the stiffness ratio of the isolators, α_K=1000. More precisely, the curves, obtained for an exterior column (figure 7a) and the interior column (figure 7b), are compared with the corresponding level of the balanced-failure load N_b.

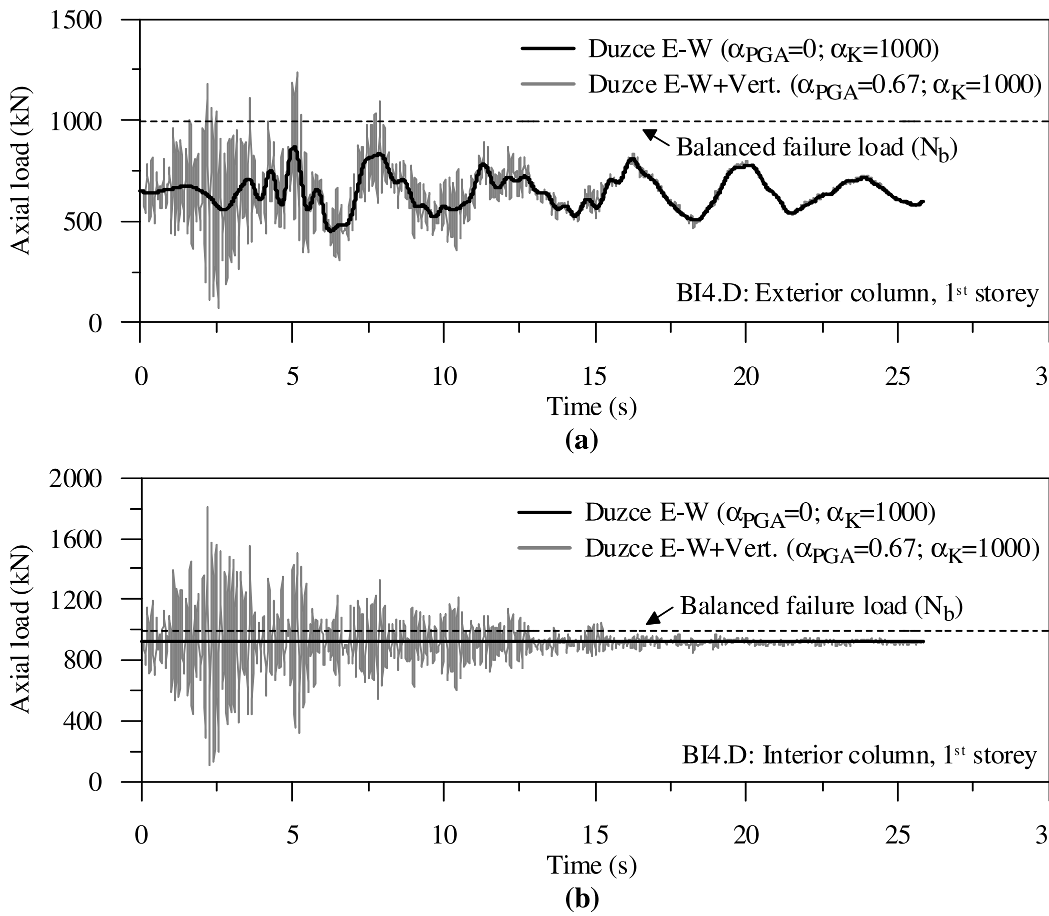

Figure 7: Time history of the axial load obtained for first-storey columns.

Due to the structural symmetry, when neglecting the vertical component of motion (i.e., assuming α_{PGA}=0), the axial load for an interior column is practically constant (exactly, if the frame structure remains elastic), while it can be observed a variation of the axial load for the exterior columns; although this last axial load shows a maximum variation equal to about 34% of the axial load induced by the gravity loads, N_{grav} (i.e., the axial load at the beginning of the time history), it does not exceed N_b.

A marked increase of the axial-load variation occurs when the vertical component of the recorded Duzce motion (α_{PGA}=0.67) is taken into account: in both the interior and exterior columns of the first storey, the axial load reaches a value of about twice as large as the corresponding N_{grav} value. In this regard, it should be noted that the tributary mass corresponding to an interior column is greater than that for an exterior column; thus, the seismic effects due to the vibrations along the vertical direction in the interior column are greater than those in an exterior column. On the contrary, the overturning moment due to the horizontal seismic loads induces an axial-load variation in the exterior columns, while practically does not affect the axial load in the interior column. Moreover, it can be observed that the interior and exterior columns present a comparable value of the balanced-failure load N_b, but this value is exceeded much more for the interior column, where the gravity axial load N_{grav} is greater than that for an exterior column.

In figures 8a and 8b it is reported the time history of the axial load in an exterior isolator (figure 8a) and in the interior one (figure 8b) of the structure BI4.D subjected to the recorded E-W and vertical components of the Duzce motion, assuming isolators deformable (i.e., α_K=1000) or rigid (i.e., $\alpha_K \rightarrow \infty$).

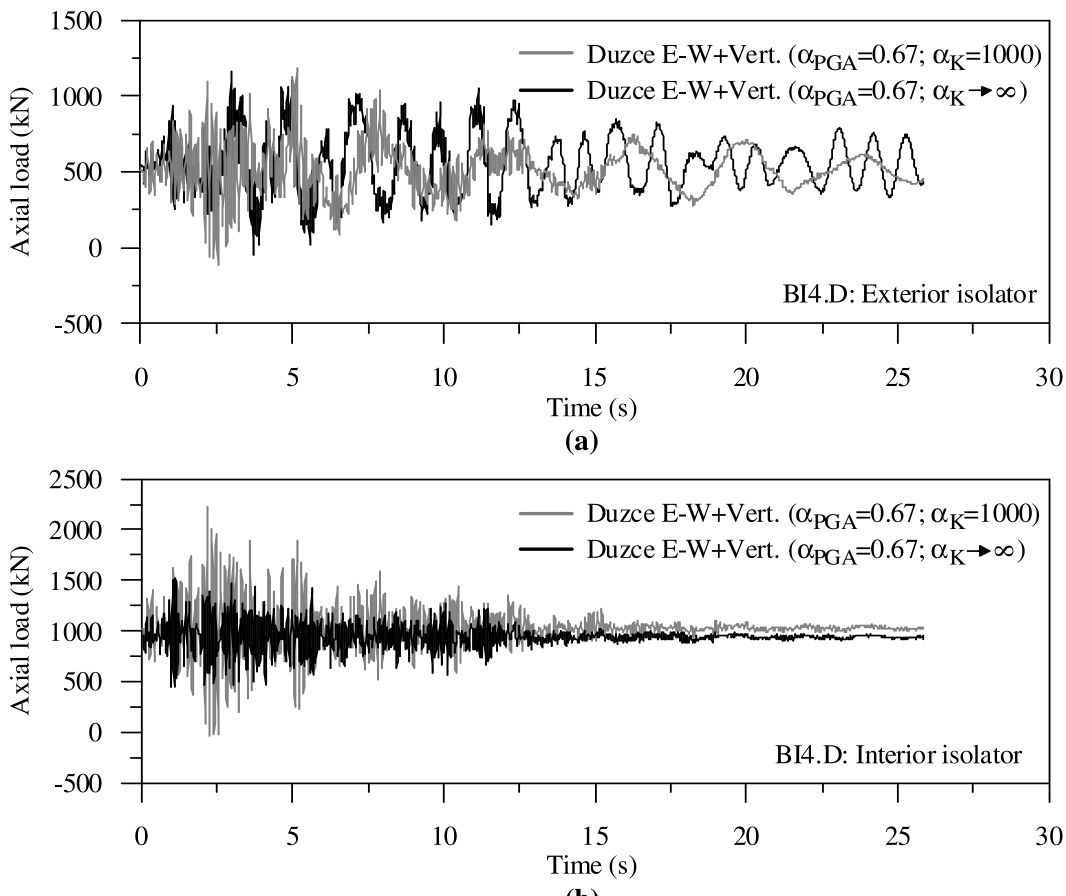

Figure 8: Time history of the axial load obtained for isolators.

For both interior and exterior isolators it is important to account for the vertical deformability: indeed, when neglecting this deformability ($\alpha_K \rightarrow \infty$), it comes out that the maximum value of the axial load is underestimated, especially for the interior isolator.

In order to evaluate the local damage undergone by the critical end sections of the r.c. frame members, the ductility demand for girders and that for columns of the BI4.D structure, when assuming α_K=1000, are respectively shown in figures 9 and 10 for different values of the acceleration ratio α_{PGA}. More precisely, the results have been obtained considering the N-S and vertical components of the Izmit-YP earthquake (figures 9a and 10a), or the E-W and vertical components of the Duzce earthquake (figures 9b and 10b). At each storey, the ductility demand is shown for the end sections of girders corresponding to exterior and interior joints (figures 9a and 9b), and for exterior and interior columns (figures 10a and 10b).

It can be observed that, even when the vertical component of motion is not considered (α_{PGA}=0), the ductility demands are rather high, especially for the Izmit-YP earthquake (figures 9a and 10a), although the test structures were designed assuming the behaviour factor q=1. Moreover, it can be noted that generally the highest values of the ductility demand have been attained for the girder sections corresponding to exterior joints (figures 9a and 9b) and for the exterior columns (figures 10a and 10b). In all the examined cases, the recorded vertical component (corresponding to α_{PGA}=0.77 or 0.67, respectively for the Izmit-YP earthquake or the Duzce one) does not produce a marked variation of the ductility demand in comparison with the case in which the same component is neglected (α_{PGA}=0). Lastly, figures 9 and 10 emphasize that the vertical component of motion, even assuming increasing values of α_{PGA}, does not produce unfavourable effects in all the cases, because this depends on how the combined characteristics of the horizontal and vertical components of the ground motion interact with the dynamic properties of the structure. It is interesting to observe that the motions corresponding to the two selected earthquakes produce different effects: indeed, an increase of α_{PGA} proves to be favourable in many cases when considering the Izmit-YP earthquake (figures 9a and 10a), whereas it is generally unfavourable with reference to the Duzce earthquake (figures 9b and 10b).

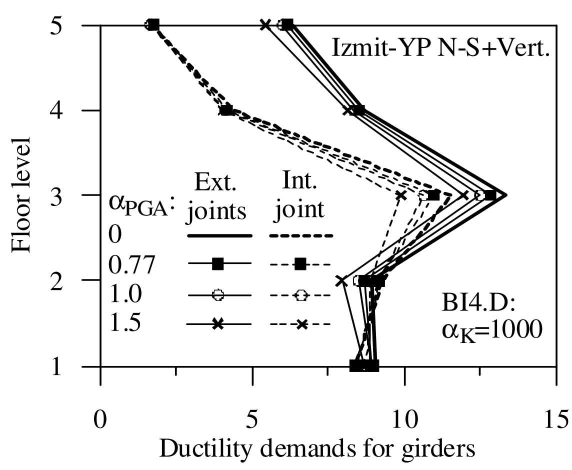

(a)

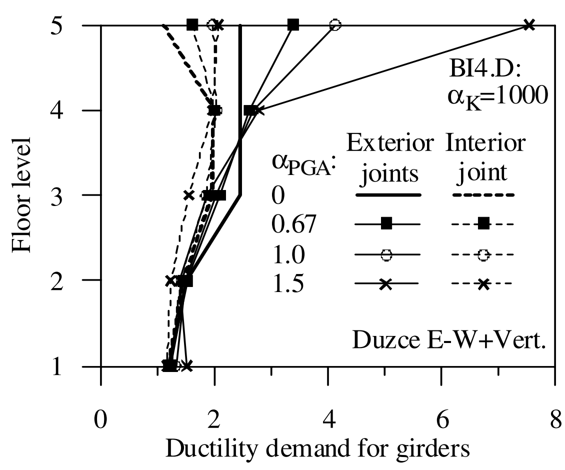

(b)

Figure 9: Ductility demand for girders assuming different values of the acceleration ratio (α_{PGA}).

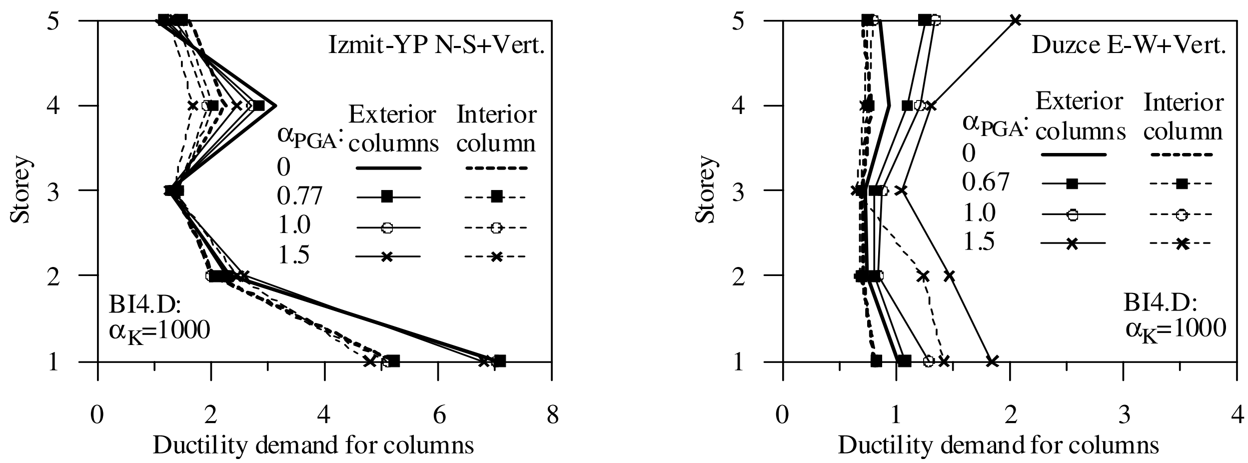

(a) **(b)**

Figure 10: Ductility demand for columns assuming different values of the acceleration ratio (α_{PGA}).

CONCLUSIONS

The effects due to the combination of the vertical and horizontal components of near-fault ground motions on the nonlinear dynamic response of a five-storey r.c. framed structure isolated at the base were investigated. The effects of the vertical component of motion were emphasized considering cases in which a horizontal component of motion is assumed acting alone or contemporaneously with the vertical one so as recorded or amplified by means of suitable values of the acceleration ratio α_{PGA}.

The results showed that, when the vertical component of the ground motion is taken into account, the isolators can undergo tensile loads. Moreover, for increasing α_{PGA} values, the variation of the axial load is evident and, for a same increase of α_{PGA}, it is more marked for the interior isolators, whose vertical stiffness has been assumed twice as large as that of the exterior isolators. The time history of the axial load emphasized that this load in the isolators (especially in an interior one) is underestimated when the vertical deformability of the isolators is neglected ($\alpha_K \rightarrow \infty$).

With regard to the r.c. framed superstructure, the results proved that the vertical component of the ground motion can induce a significant variation of the axial load in the columns: when assuming increasing α_{PGA} values, the axial load can reach even the ultimate load in compression (with brittle failure) or in tension. In all the examined cases, when considering the recorded vertical ground motion, the compressive load exceeded that corresponding to the balanced failure, at all the storeys, except at the top storey; on the contrary, the ductility demand for all the r.c. frame members exhibited a small variation in comparison with the case in which the vertical component of motion was neglected. Lastly, the vertical component of motion, even assuming increasing values of α_{PGA}, did not produce unfavourable effects on the ductility demand in all the cases (in some cases produced even a favourable effect), because this depends on how the combined characteristics of the horizontal and vertical components of the ground motion interact with the dynamic properties of the structure.

The present work was partially financed by M.I.U.R.
(Italian Ministry of the Education, University and Research).

REFERENCES

1. Alaghebandian R, Otani S, Shiohara H. “Effect of distributed mass on earthquake response of reinforced concrete frames.” Proceedings of the 12th World Conference on Earthquake Engineering, Auckland, New Zealand, 2002. Paper no. 2230.
2. Decanini LD, Liberatore L, Mollaioli F. “Response of bare and infilled rc frames under the effect of horizontal and vertical seismic excitation.” Proceedings of the 12th European Conference on Earthquake Engineering, London, UK, 2002. Paper no. 164.
3. Morishita M, Kato A, Yabana S, Fujita T. “The seismic protection of nuclear facilities: main requirements and benefits of using isolation and progress of related R&D in Japan.” Proceedings of the 7th International Seminar on Seismic Isolation, Passive Energy Dissipation and Active Control of Vibrations of Structures, Assisi, Italy, 2001. Paper no. L04.
4. Kelly JM. “The role of damping in seismic isolation.” Earthquake Engineering and Structural Dynamics 1999; 28: 1717-1720.
5. Benedetti D, Carydis P. “Influence of the vertical component on damage during shallow – near field earthquakes.” European Earthquake Engineering 1999; 3: 3-12.
6. Papazoglou AJ, Elnashai AS. “Analytical and field evidence of the damaging effect of vertical earthquake ground motion.” Earthquake Engineering and Structural Dynamics 1996; 25: 1109-1137.
7. Eurocode 8. “European Standard, Design of structures for earthquake resistance. Part 1: General rules, seismic actions and rules for buildings.” Draft no. 6, 2003.
8. Salazar AR, Haldar A. “Structural responses considering the vertical component of earthquakes.” Computer and Structures 2000; 74: 131-145.
9. European Commission for Community Research. “European Strong motion Database” (on-line). www.isesd.cv.ic.ac.uk/ESD.
10. Uang C-M, Bertero VV. “Evaluation of seismic energy in structures.” Earthquake Engineering and Structural Dynamics 1990; 19: 77-90.
11 Ordinanza n. 3274, President of the Italian Council of Ministers. “First elements about the general criteria for the seismic classification of the national territory and the technical rules for aseismic constructions. Annex 2: Technical rules for the design, assessment and seismic retrofitting of the buildings.” 2003 (in Italian).
12. Mazza F, Vulcano A. “Base-isolation techniques for the seismic protection of rc framed structures subjected to near-fault ground motions.” Proceedings of the 13th World Conference on Earthquake Engineering, Vancouver, Canada, 2004. Paper no. 2935.
13. Vestroni F, Vulcano A, Di Pasquale G. “Earthquake response analysis of a nonlinear model of a base-isolated structure.” Proceedings of the International Meeting on Earthquake Protection of Buildings, Ancona, Italy, 1991; 181/C-190/C.
14. Mazza F, Vulcano A. “Seismic response of buildings with isolation & supplemental dissipation at the base.” Proceedings of the 5th World Congress on Joints, Bearings and Seismic Systems for Concrete Structures, Rome, Italy, 2001; CD-ROM.